Gil-González, Nerea; Benito-Lopez, F.; Castaño, E.; Morant-Miñana Maria C. (2020). **Electrical and electrochemical properties of imidazolium and phosphonium-based NIPAAM ionogels**. Electrochimica Acta, 345 : 136167
https://doi.org/10.1016/j.electacta.2020.136167.

Electrical and electrochemical properties of imidazolium and phosphonium-based pNIPAAM ionogels

Nerea Gil-González[1,2], F. Benito-Lopez[3], E. Castaño[1,2], Maria C. Morant-Miñana[4,*]

[1]*Ceit, Manuel Lardizabal 15, 20018 Donostia / San Sebastián, Spain*

[2]*Universidad de Navarra, Tecnun, Manuel Lardizabal 13, 20018 Donostia / San Sebastián, Spain*

[3]*Analytical Microsystems & Materials for Lab-on-a-Chip (AMMa-LOAC) Group, Microfluidics Cluster UPV/EHU, Analytical Chemistry Department, University of the Basque Country UPV/EHU, Spain*

[4]*Centre for Cooperative Research on Alternative Energies (CIC energiGUNE), Basque Research and Technology Alliance (BRTA), Alava Technology Park, Albert Einstein 48, 01510 Vitoria-Gasteiz, Spain.*

Corresponding author: mmorant@cicenergigune.com

Abstract

The electrical and electrochemical properties of two ionogel materials based on the poly(*N*-isopropylacrylamide) gel with 1-ethyl-3-methylimidazolium ethyl sulfate and trihexyltetradecyl-phosphonium dicyanamide ionic liquids are investigated. The current-voltage curves show a current rectification for both ionogels and ionic liquids after inducing ion adsorption on gold electrode surface. The polymer matrix of the ionogels mitigates ion adsorption, resulting in lower rectification ratios when comparing with the corresponding ionic liquids. The stability and the electrochemical window (ECW) of the ionogels are calculated from cyclic voltammograms and compared with the ones obtained for the ionic liquids, achieving the widest electrochemical window the phosphonium based ionic liquid and its ionogel. Finally, the effect of the absorbed atmospheric water and the coefficient diffusion of the redox active species inside the IO is calculated. This

work widens the knowledge of the behavior of ionogel materials characterized on gold electrode interfaces.

Keywords: Ionogel (IO); ionic liquid (IL); current rectification; electrochemical window (ECW); interdigitated electrodes (IDEs).

1. Introduction

Ionogels (IOs) are a class of hybrid materials that consist of ionic liquids (ILs) immobilized into a matrix. Inorganic, hybrid and organic matrices can be employed to prepare different types of IOs. Among them, polymer-based IOs can be prepared by solution of the polymer and the IL in a co-solvent which is removed (solvent blending), by swelling of the polymer in IL (impregnation) or in situ polymerization of monomer dissolved in the IL. As a consequence, the different physical or chemical properties of both components are combined, resulting in a material that differs from their original components.[1] The intrinsic ionic conductivity of the IL and the mechanical and shape stability of its matrix designate IOs as interesting materials for the fabrication of electrochemical devices, where a high ionic conductivity, at the solid state, generates safer and lighter devices.[2] The incorporation of ILs with different anions and cations within the matrix of a polymeric material provides a path for an easy tuning or tailoring of the properties of the IO and allows the fabrication of functional devices such as batteries and fuel cells.[3] These properties are not present in hydrogels where the ionic liquid has been substituted by water. In fact, its major drawback is derived from its high water content that makes them weak and causes them a rapidly moisture loss, shrinkage and brittleness.[4]

In particular, poly(*N*-isopropylacrylamide) (pNIPAAM) IOs that utilize imidazolium- or phosphonium-based ILs are flexible materials with easily tunable appearance. Imidazolium-based ILs are moisture stable, do not undergo hydrolysis, have low melting points and good thermal stability which make them one of the most stable, common and studied ILs family.[5] On the contrary, phosphonium-based ILs are less studied materials with interesting properties such as its high hydrophobicity and stability against high temperatures (up to 400ºC) and basic pH solutions. Both materials have traditionally been employed as microvalves[6,7] and passive pumps actuators[8,9] as well as for pH monitoring,[10] in microfluidic devices. These materials have been fully characterized by DSC, SEM,[11] optical microscopy[9] and AFM.[12] However, a less considered aspect of these materials are their electrical and electrochemical properties.

Recent studies in our group have demonstrated that the actuator behavior of these thermo-responsive IOs can be studied with electrochemical impedance spectroscopy (EIS) and that the charge-transfer resistance of the IOs can be correlated with the morphological properties of the IL included in the IO. Using this technique, the time necessary for the formation of the network during the photopolymerization process and the water uptake of both IOs was determined.[12] In addition, a better understanding of the actuation behavior of the IOs was provided with repeated drying and swelling cycles employing either gold or AZO-based interdigitated electrodes.[13] In addition, the quasi-solid nature of these electrolytes makes them a suitable alternative to circumvent the current problems derived from the use of liquid electrolytes in several applications such as gas sensors[14,15], supercapacitors, batteries and solar cells.[16] Regarding to supercapacitors, those commercially available are composed of two activated carbon electrodes and a porous separator soaked by a liquid electrolyte. The IOs can be implemented as separator and electrolyte and fulfil the safety requirements.[17] In the

field of batteries, the lithium-ion secondary (rechargeable) batteries are the most studied battery types. Unfortunately, they present a safety problem due to the highly flammable components of electrolytes. IOs are promising electrolytes to circumvent this problem. Moreover, these electrolyte systems do not require the use of the conductive salt (ex. $LiPF_6$) that easily releases toxic compounds when the battery is damaged.[18]

With the rapid growth of electronic industry, these materials can be also implemented in electronic applications such as rectifiers. The deposition of the IO onto an electrode forms a metal-semiconductor contact that can be classified as Ohmic (current proportional to the applied voltage) or non-Ohmic (with a rectification behavior). In this context, the synthesis of hydrogels doped with oppositely charged ions to generate *n*-type and *p*-type regions has been investigated,[19] achieving current rectification ratios as large as 40 mA cm^{-2} and current densities up to 50 mA cm^{-2}. For instance, acrylamide in the presence of pyranine as *p*-type hydrogel and *N*-isopropylacrylamide in the presence of 3-methacrylamido-*N,N,N*-trimethylpropan-1-aminium chloride as *n*-type hydrogel have been polymerized and studied.[20] It was observed that, after placing one of the gels on the top of the other, rectification current was achieved. These junctions are cheaper and simpler to fabricate than inorganic *p-n* junctions, however their main disadvantage is that they include water and, over time, they will stop rectifying. This drawback has been solved with the replacement of hydrogels by IOs. As an example, Nayak *et al*.[21] fabricated and Schottky diode with pristine and 1-butyl-3-methylimidazolium chloride ([BMI][Cl]) or 1-butyl-3-methylimidazolium hexafluorophosphate ([BMI][IPF_6]) ILs dispersed in PEDOT:PSS using Au and Al electrodes. However, in order to mimic silicon-based technologies, new electronic and electrochemical devices, employing conducting IOs as active materials, are an interesting option to enhance their performance and

overcome the current limitations of existing devices in terms of cost, fabrication methods and thermal and electrochemical instabilities.

Here we report an easy fabrication process to study the influence of two ILs, 1-ethyl-3-methylimidazolium ethyl sulphate ($[C_2mIm][EtSO_4]$ (IL-1) and trihexyl(tetradecyl)phosphonium dicyanamide ($[P_{6,6,6,14}][DCA]$) (IL-2), on the electrical and electrochemical performance of pNIPAAM based IOs. The rectification behavior, employing current-voltage (I-V) curves, has been investigated for two IOs with different physicochemical properties. In addition, the electrochemical stability, the effect of the absorbed atmospheric water in the IOs and the mass transport of electroactive molecules inside the IO have been investigated by cyclic voltammetry (CV). The results have been compared with the neat ILs, thus widening the knowledge about the electrical and electrochemical conducting IOs with different polarities tuned by encapsulating different ILs in the polymeric matrix.

2. Experimental

2.1. Reagents and materials.

N-isopropylacrylamide, *N,N'*-methylene-bis(acrylamide), 2,2-Dimethoxy-2 phenylacetophenone, potassium ferricyanide ($K_3[Fe(CN)_6]$), 1-ethyl-3-methylimidazolium ethyl sulfate IL and trihexyltetradecyl-phosphonium dicyanamide IL were purchased from Sigma-Aldrich. Cyclic olefin copolymer (COP) was provided by Zeonex/Zeonor and pressure sensitive adhesive (PSA) was gently provided by Adhesive Research, Ireland. Demineralized water was taken from a Mili-Q Plus purification system with a resistivity of not less than 18 MΩ cm.

2.2. Synthesis of the ionogels.

The composition of the IOs employed is based in the synthesis conditions previously described in the literature.[6–9] A mixture of N-isopropylacrylamide (0.904 g), N,N′-methylene- bis(acrylamide) (0.025 g), 2,2-dimethoxy-2-phenylacetophenoneand (2 mL) 1-ethyl-3-methylimidazolium ethyl sulfate (IO-1) or trihexyltetradecyl-phosphonium dicyanamide (IO-2) ionic liquid was placed in a flask and heated at 80 °C during 30 min. The chemical structures of the IOs used in this study are shown in the Supporting Information (SI), Figure S1.

2.3. Fabrication of the electrochemical device, and integration with the IOs

The fabrication of gold interdigitated electrodes (Au-IDEs) has been previously described.[22,23] In brief, a 200 nm gold layer was deposited by RF magnetron sputtering (Edwards coating system E306A) in an argon (Ar) atmosphere onto positive photoresist previously patterned employing a photolithographic process. An 8 nm layer of titanium (Ti) as adhesion layer was deposited by DC magnetron sputtering. The rest of the photoresist was washed away using a lift-off process and devices with interdigitated electrodes of 50 μm width, 11 fingers and 950 μm finger overlap were obtained.

Electrochemical treatment of gold electrodes in sulphuric acid (0.05 mM) was performed to clean and prepare the surface of the electrodes prior depositing the IOs. After that, the electrode was cleaned with acetone and ethanol and dried in N_2. Finally, 1 μL of IO-1 or IO-2 was drop-casted and *in situ* photopolymerized for 8 min onto the Au-IDEs under UV light at 365 nm (850 μW cm^{-3}) using a COP/PSA gasket to stablish the IO boundary.

2.4. Characterization methods

Cyclic voltammetry measurements were recorded with a symmetrical two-electrode system using an electrochemical analyser (CH Instruments Model 1040B). For the

electrical characterization a Keithley 2450 Sourcemeter was used. The electrodes were connected with needles controlled by micro positioners (see SI, Figure S2).

3. Results and discussion

3.1. Electrical characterization of IOs and ILs

Current-voltage (I-V) measurements were performed on not induced devices, which accommodate two interdigitated electrodes with two connection pads onto a thermally oxidized (1.4 μm) silicon wafer. In the first experiment, both IOs were measured without any prior voltage history at room temperature. Figure 1(a) shows that the I-V curves of both IOs present a non-linear symmetric behavior with a rectification ratio ($I_{+1\ V}/I_{-1\ V}$) near unity (see Table 1). At 1V, the conductivity values are $1.47 \cdot 10^{-7}$ and $8.40 \cdot 10^{-8}$ S cm^{-1} for IO-1 and IO-2, respectively. The conductivity[24] was calculated from equation 1,

$$\sigma = \frac{2}{N \times L \times R} \qquad \text{(Equation 1)}$$

where N is the number of finger electrodes, L is finger overlap and R is the resistance value measured at 1 V.

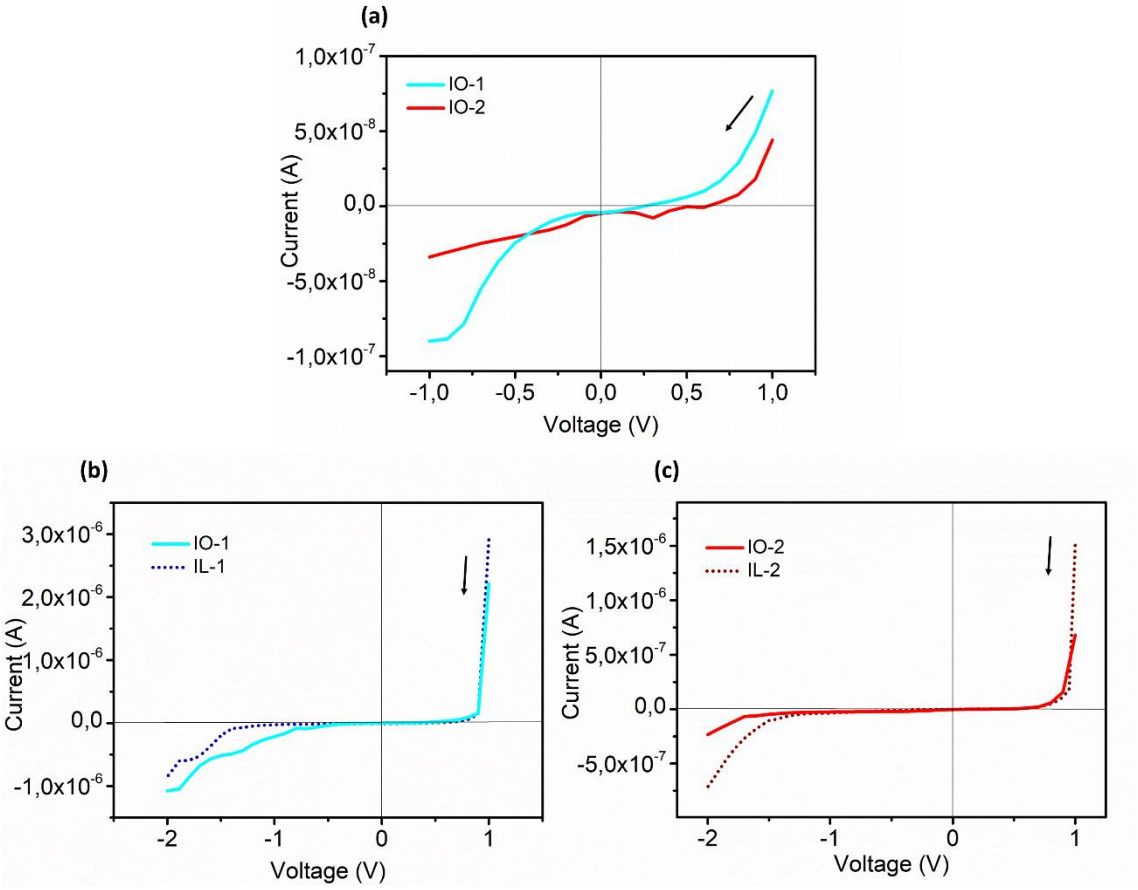

Figure 1. (a) I-V curves of not induced devices prepared IO-1 and IO-2; (b) I-V curves of IO-1 and IL-1 after applying 3 V; (c) I-V curves of IO-2 and IL-2 after applying 3 V. The arrows point the scan direction.

As expected, IO-1 presents higher conductivity than IO-2 due to the higher mobility of imidazolium cation[25] which is related to its lower viscosity and its smaller Stokes radius in comparison to the phosphonium cations present in IO-2.[26] For the phosphonium-based IO-2, the electrophoretic mobility is much lower, which might result from the combination of two effects: the long alkyl chain length of the cation[27] and the preferential interactions between the cation and the anion of the IL.[28]

Table 1. Conductivity values, current and rectification ratios of not induced and voltage induced active materials.

Entry	Active	Voltage induced	Current	Current	Rectification

	material	device[a]	(A)[b]	(A)[c]	ratio[d]
1	IO-1	no	$7.68 \cdot 10^{-8}$	$-8.79 \cdot 10^{-8}$	0.88
2	IO-2	no	$4.39 \cdot 10^{-8}$	$-3.48 \cdot 10^{-8}$	1.26
3	IO-1	yes	$2.22 \cdot 10^{-6}$	$-2.18 \cdot 10^{-7}$	12.33
4	IL-1	yes	$2.90 \cdot 10^{-6}$	$-2.83 \cdot 10^{-8}$	102.47
5	IO-2	yes	$6.74 \cdot 10^{-7}$	$-2.62 \cdot 10^{-8}$	25.72
6	IL-2	yes	$1.50 \cdot 10^{-6}$	$-3.76 \cdot 10^{-8}$	39.89

[a]Devices scanned from 0 to -3 V prior to recording I-V plots; [b]Current at +1 V; [c]Current at -1 V; [d]Ratio between the absolute current at ±1 V.

Interestingly, if an initial sweep was carried out from 0 V to -3 V and, subsequently, form +1 V to -2 V (Figure 1(b)) a current increase of two order of magnitude was observed in IO-1 at +1 V when compared to the not induced device (Table 1). Moreover, as the voltage was swept towards -2 V, the absolute value of the current was lower than the obtained in the non-voltage-induced device originating an asymmetric behavior with a current rectification ratio of 12.33 at ±1 V. This behavior could be explained because without any applied voltage, the anions mix with the cations to obtain a charge compensation and when the I-V plot is recorded, the ions move to the opposite charged electrode resulting in the symmetric I-V curve illustrated in Figure 1(a). In addition, the adsorption of IL ions on metal electrodes with changes in the applied voltage has been previously reported.[29–31] Therefore, we hypothesize that the induced current rectification could be explained by the adsorption of ions onto Au surface that generates an accumulation zone and consequently an asymmetric I-V curve.

To study the role of the polymer matrix in the IO-1, the I-V curve for IL-1 was recorded following the previously explained procedure. Figure 1(b) shows that the I-V curve recorded for IL-1 presents also a very pronounced voltage induced asymmetric behavior with higher rectification ratio than IO-1 at ±1 V (Table 1). Although, IO-1 presents a porous matrix that allows ion motion between the electrodes,[12] the number of ions in contact with electrode surface is higher in neat IL which could increase the number of

adsorbed ions on the electrode. The induced behavior is reproducible, since this response occurs each time that we applied the external input, but the rectification behavior is not maintained with time and the rectification effect is reduced over the cycling time (see figure S3).

The same procedure was repeated for IO-2 and IL-2; see Figure 1(c). Similar to IO-1, after applying a voltage swept, the symmetric I-V curve obtained in the not induced device (Figure 1(a)) changed to an asymmetric behavior with higher rectification ratio for the neat IL than the IO-2. Rectification ratios of 25.72 and 39.89 were calculated for IO-2 and IL-2, respectively. Lower currents were observed for IO-2 than for IL-2 pointing out that the compact matrix formed during the photopolymerization hindered ion motion towards electrode surface. However, these differences were less pronounced than in the case of IO-1 and IL-1 due to their so markedly different physical properties among imidazolium- and phosphonium-based ILs, which are the key components of the ionogels properties.

3.2. Study of the electrochemical properties of ILs and IOs

A general common feature of ILs is their inherent redox robustness, which allows them to carry out a variety of functions.[32] To investigate the electrochemical properties of ILs and IOs, first, cyclic voltammetry (CV) measurements were carried out at room temperature. CV offers a rapid location of redox potentials and evaluation of the effect of media on the redox processes. Prior to CV measurements, the surface of the bare electrodes was electrochemically activated in diluted H_2SO_4 to produce a clean and uniform metallic surface with a thin uniform oxide layer on the metal.[33,34] The electrodes were cycled until a reproducible fingerprint was obtained (see SI, Figure S4).

After the activation of the gold surface, the electrodes were washed and either IL or IO was polymerized onto the surface.

The stability of IL-1 and IL-2 against redox processes was evaluated from -2 V to -3.7 V and from -2 V to -4 V, respectively. For IL-1 a reduction peak appeared at -3.38 V, which was assigned to the irreversible reduction peak of the imidazolium cation,[35,36] see Figure 2(a). In the case of IL-2, an irreversible reduction peak of the phosphonium cation[37] was observed at -2.9 V, see Figure 2(b). The measurements were repeated for IO-1 and IO-2. The reduction peak in IO-1 was slightly shifted towards lower values (-3.42 V). In the case of IO-2, the reduction peak appeared at similar voltage to IL-2 (-2.89 V) showing a little effect of the polymeric matrix. The absence of reactions until high potentials proves the robustness of the IOs and shows their applicability for the design and fabrication of a vast number of electrochemical devices.

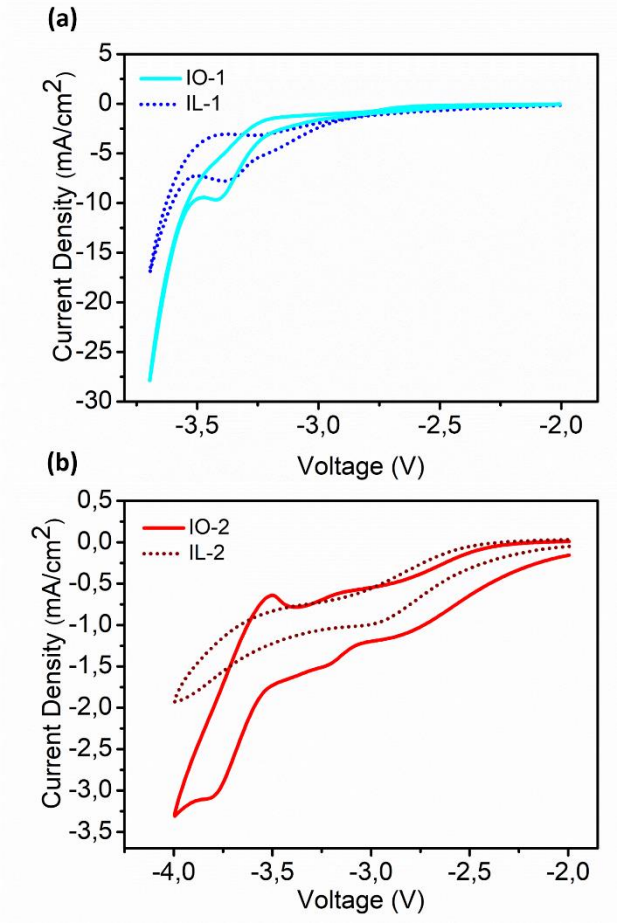

Figure 2. Cyclic voltammograms of (a) IO-1 and IL-1 between -2 V and -3.7 V and for (b) IO-2 and IL-2 between -2 V and -4 V at 0.1 V s^{-1}.

Water is one of the most significant impurities present in ILs, which can be absorbed during storage or manipulation of the device. In order to further evaluate the performance of the IOs after atmospheric water uptake, IOs and ILs were deposited onto Au-IDEs and stored in lab during 24 h. After that, the electrochemical potential window (ECW) and the CV of both IL and IOs were measured. The ECW is a key criterion to be considered when a medium is used in electrochemical applications.[38] The anodic and cathodic limits are determined by the oxidation of the anions and the reduction of the cations[39] and have been defined as the potential at which the current density reached 0.5 mA cm^{-2}. For the studied samples, the ECWs were determined using the voltammograms of the Figures 3(a) and 3(b). IL-1 presented an ECW of 0.59 V while IL-2 presented a value of 5.12 V. The ECW values measured are different to the values reported to IL-1 (ECW = 4.0 V) and IL-2 (ECW = 3.2 V).[40] The smaller value measured for IL-1 is probably due to the water absorption from the atmosphere.[41] On the contrary, the larger value of the IL-2 can be explained considering its hydrophobic nature, which avoids the massive uptake of water during the exposure time. The ECWs follow the same trend when the ILs are incorporated inside the polymeric matrix and IO-2 (ECW = 3.88 V) has wider potential ranges than IO-1 (ECW = 1.47 V). Although the IOs have the same anions and cations that their corresponding IL the presence of the pNIPAAM plays an important role in their electrochemical stability since interactions between the ions and the polymer chain can modify the physicochemical properties of the ILs.[42] The wider ECW of IO-1 can be related with the decrease in conductivity of the IO-1 when is encapsulated in the polymeric matrix. Although this decrease in conductivity occurs also in IO-2, the appearance of a reduction shoulder centered at 2 V could be the responsible of the

narrowing of its ECW. It is important to mention that the ECW for both IOs is wide enough for electrochemical applications and IO-2 could be suitable for those that require an open space environment.

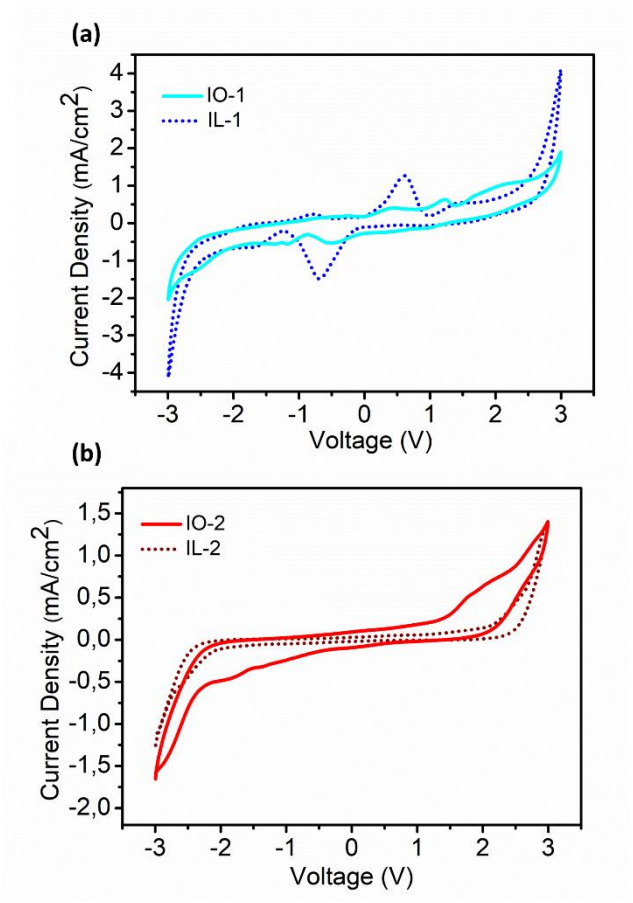

Figure 3. Cyclic voltammograms of (a) IO-1 and IL-1 and (b) IO-2 and IL-2 between -3 V and + 3 V at 0.1 V/s[1].

Figure 3(a) shows CV curves obtained with Au-IDEs in IL-1 and IO-1 in the potential range between -3 V and +3 V. The general appearance of the IL-1 voltammogram is very similar to that obtained with diluted H_2SO_4 (see SI, figure S3). The presence of peaks at -0.68 V and 0.61 V are related to the reduction and oxidation of hydrogen atoms and oxygen-containing surface species[43–45] absorbed by the moisture of the atmosphere. In IL-1 the water absorption from the air arises from the hydrogen bonding interaction between the water molecules and the sulfate groups of the anion.[37] The current intensity

of the peaks depend strongly on water concentration. In the case of IO-1, the peaks moved to -0.5 V and 0.45 V and a decrease in the peak current was observed, which can be explained by the lower ability of the IO-1 to absorb water from the atmosphere in comparison to IL-1. For IL-2 and IO-2, the peaks related to water were not observed; see Figure 3(b). This can be related with their low water solubility (molar fraction = 0.43) due to the large alkyl-chain of the cation of the IL-2. In both cases, the absence of peaks related with water proved the suitability to use IL-2 or IO-2, under open atmospheres, due to its lower ability for water uptake from atmosphere.

Imidazolium-based ILs present relatively low viscosities (96.6 mPa·s) and high conductivities, which make them of particular interest from the electrochemical point of view. Among others diffusion coefficients are very interesting parameters and can be determined by CV. Since a concentration gradient is established in the solution, the relaxation rate is governed by the mutual diffusion coefficient (D_m).[47] Therefore, IO-1 and IL-1 were selected to study the diffusion of water molecules by measuring the effect of the scan rate (υ) on the peak current (i_p). The recorded voltammograms between -1.5 V and 2.5 V with different scan rates from 0.02 V s^{-1} to 0.1 V s^{-1} are shown in Figure 4(a) for IL-1. With the increase of the scan rate, the reduction peak shifted negatively, and the oxidation peak shifted positively indicating a quasi-reversible process. The Randles-Sevcik equation predicts that the peak current at different scan rates should be proportional to the square root of the scan rate, if the reaction kinetic is controlled by diffusion conditions. At 25 ºC the Randles-Sevcik equation can be reduced to the following equation:

$$i_p = 268600 * n^{\frac{3}{2}} * A * D^{\frac{1}{2}} * C * \vartheta^{\frac{1}{2}} \quad \text{(Equation 2)}$$

where n is the number of electrons transferred in the redox reaction, A (cm^2) is the electrode surface area, D (cm^2 s^{-1}) is the D_m coefficient of the oxidized compound, i_p is the anodic peak current, υ (V s^{-1}) is the scan rate and C (mol cm^{-3}) is the bulk concentration of the analyte.[48] As shown in Figure 4(b), the plot of peak current *versus* $\upsilon^{1/2}$ yields to a straight line with a slope directly related with the D_m coefficient since the area of the electrode, the number of electrons in the reduction and the oxidation process and the water concentration were kept constant for the IL-1 and IO-1. In this particular case, slope values of $(8.336 \pm 0.497)\cdot10^{-7}$·A·s V^{-1} and $(-1.993 \pm 0.172)\cdot10^{-6}$ A s V^{-1} were obtained for the anodic and cathodic peaks, respectively. In the case of IO-1, the voltammograms measured with scan rates from 0.02 V s^{-1} to 0.1 V s^{-1} showed a decrease in the peak current compared to IL-1 (Figure 4(c)). Moreover, the linear relationship of the peak currents versus $\upsilon^{1/2}$ suggests that in this case the reaction is also governed by the diffusion (figure 4(d)). The slope values for IO-1 were $(8.557 \pm 0.038)\cdot10^{-7}$ A s V^{-1} and $(-1.120 \pm 0.155)\cdot10^{-7}$ A s V^{-1}, showing a lower water diffusion in comparison with the neat IL. *Zao et al.*[45] proved that higher hydrophobicity/viscosity values protect the material from the experimental environment. In the case of bis(2-hydroxyethyl)-ammonium acetate ([DEA][Ac]), the higher viscosity values (336 mPa·s) were related with the lower slope values (ca. 10^{-7} A/ppm) obtained using the stripping peak current by using the standard addition method of water in a dried IL. On the contrary, triethylammonium acetate ([TEtA][Ac]), with a viscosity value of 11 mPa·s present higher slope values (ca. 10^{-6} A/ppm). Moreover, our results, prove that the same behavior is achieved by the polymeric matrix, that makes the IL less reactive with water without the need of using hydrophobic or highly viscous anions.

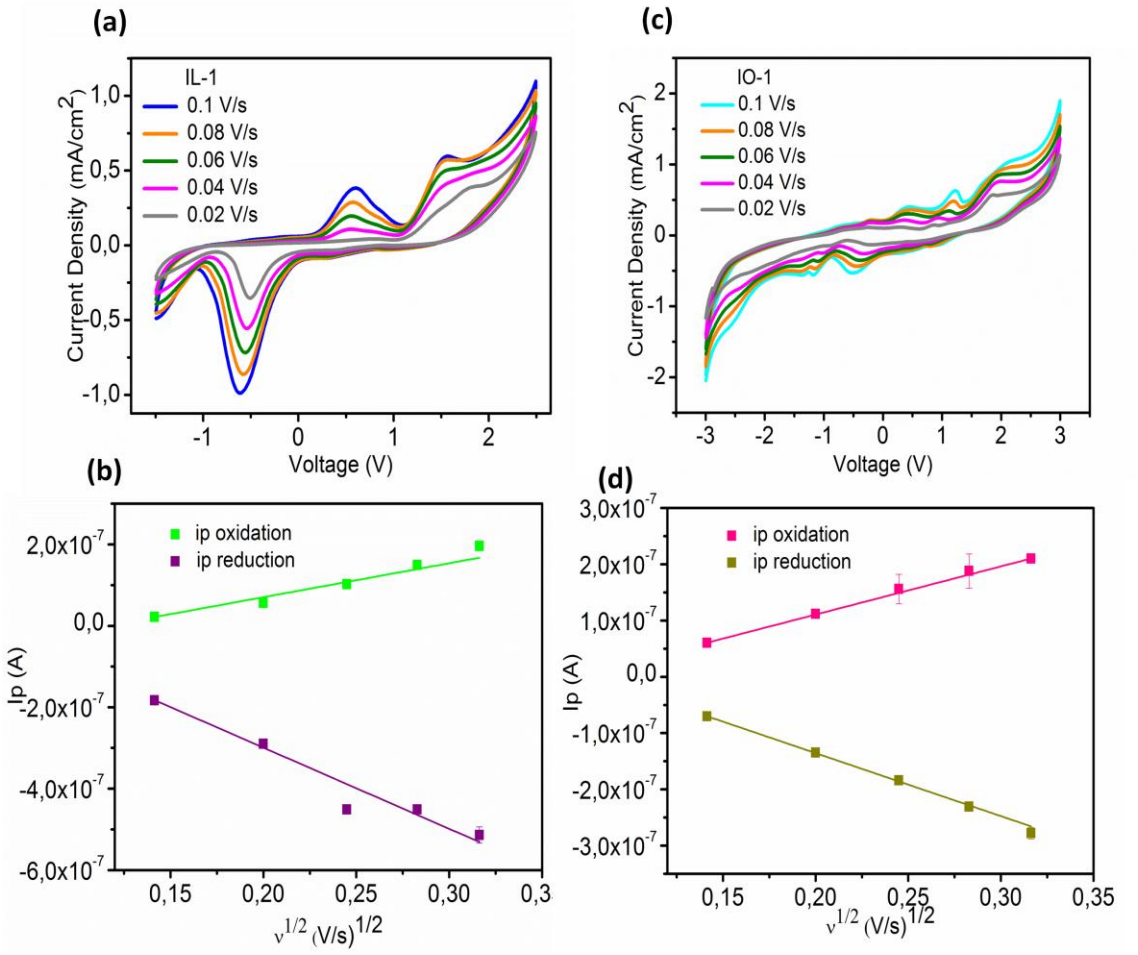

Figure 4. (a) Cyclic voltammogram of IL-1 between -1.5 V and 2.5 V at different scan rates. (b) Oxidation (0.61 V) and reduction (-0.68 V) peak currents of IL-1 *vs* scan rate^1/2. (c) Cyclic voltammogram of IO-1 between -3 V and +3 V. (d) Oxidation (-0.5 V) and reduction peak (0.45 V) currents of IO-1 *versus* scan rate$^{1/2}$.

IL can be also employed as electrochemical solvents, but their special characteristics directly impact in the voltammetric behavior of the species dissolved in the IL. For this particular use, the mass transport of electroactive analytes in ILs to the electrode interface is an interesting parameter. The rate of mass transport is mainly determined by viscosity but in ILs, the D_m coefficients of redox pairs are often inequal.[49] D_m coefficients of redox pairs in IO-1 were calculated using CV at microelectrodes employing the ferro/ferricyanide redox couple, $[Fe(CN)_6^{3-/4-}]$ without the need of attaching the

ferrocene to the imidazolum center or acting as a counterion. pNIPAAM swells in presence of an aqueous solution and the hydrophilic IL of IO-1 enhances water absorption as observed in the previous results. Therefore, taking advantage of this property, IO-1 was immersed in a potassium ferricyanide ($K_3Fe(CN)_6$) solution during 5 min until it presented a homogeneous yellow color. After that, a cyclic sweep between -0.75 V and +0.75 V was carried out employing a scan rate of 0.1 V s^{-1} as can be seen in Figure 5(a). CV measurements of IO-1 showed a pair of quasi-reversible peaks attributed to the Fe^{+3}/Fe^{+2} redox couple. Thus, the one electron transfer process for ferro/ferricyanide redox couple found in many organic solvents also occurs in an IO with the absence of supporting electrolyte.

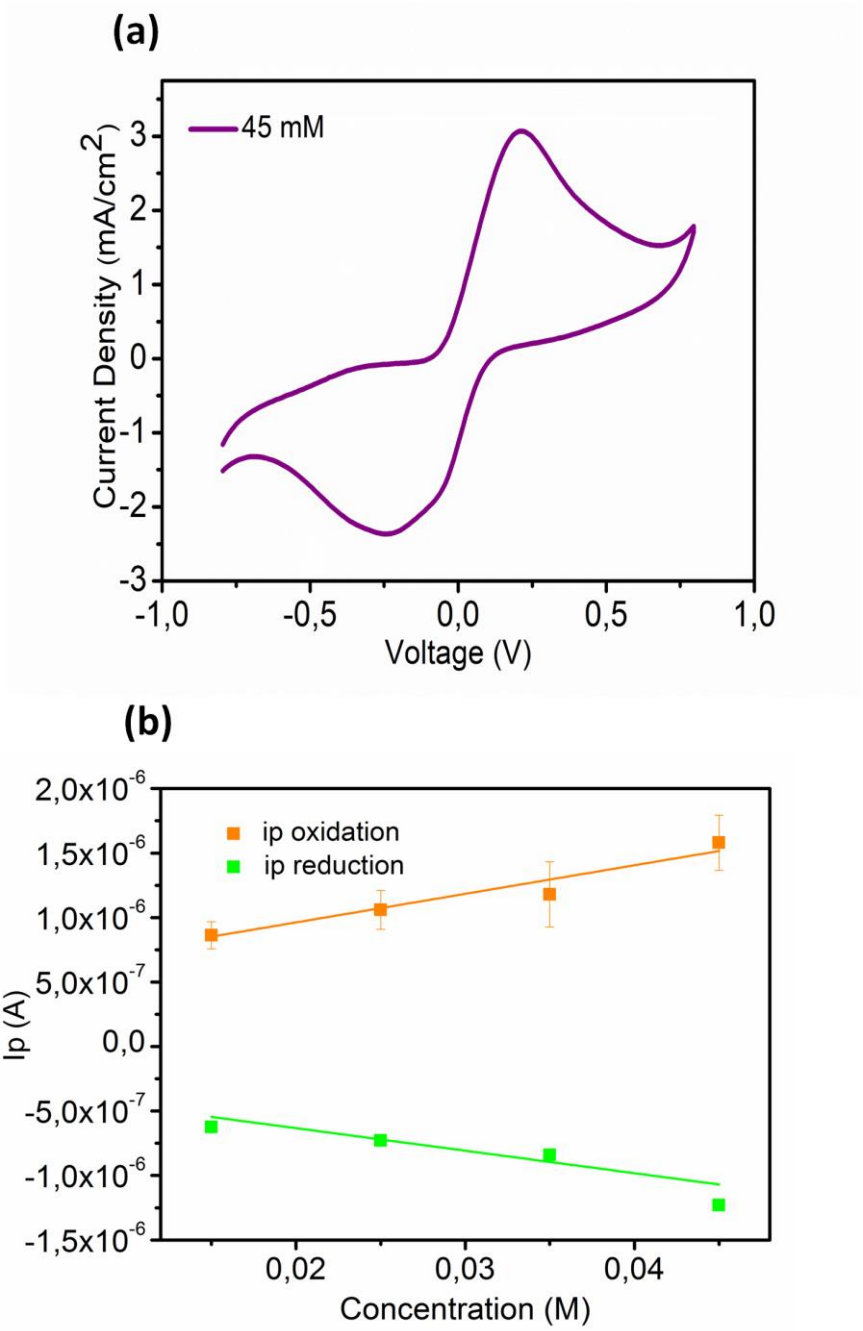

Figure 5. (a) Cyclic voltammograms of IO-1 at 0.1 V/s after swelling in $K_3Fe(CN)_6$ solution. (b) The dependence of oxidation and reduction peak currents on $K_3Fe(CN)_6$ concentration.

The intensity of the peak current was measured at various concentrations ranging from 15 mM to 45 mM using a scan rate of 0.1 V/s (see SI, Figure S5) and the current of the anodic and the cathodic peaks are plotted in Figure 5(b). The linearity of the plot suggests

that the electrode reaction kinetics is controlled by the diffusion conditions in the studied concentration range. Moreover, using the Randles Sevcik equation, it is possible to calculate the diffusion of $Fe(CN)_6^{3-/4-}$ through the IO-1. A D_m coefficient of $(7.954\pm0.153)\cdot10^{-15}$ cm^2 s^{-1} was calculated, which is significantly smaller than the diffusion of the redox couple measured onto bare electrodes ($2.71\cdot10^{-6}$ cm^2 s^{-1}).[50] The D_m coefficient for the cathodic peak is $(6.191\pm0.726)\cdot10^{-15}$ cm^2 s^{-1}, which means that the ratio between the coefficients of the redox pair is near to 1 showing little interaction between the imidazolium cation and the structure of the diffusing species.[51] Therefore, IO-1 does not inhibit the diffusion of the electroactive species, despite the high viscosity of the IL-1, and provides an ideal environmentally benign experimental platform for the study of electroactive redox molecules without employing binary mixtures of linking the electroactive ferrocene unit to the imidazole cation.[52] Moreover, the combination of IOs with microelectrode systems provides a large range of possibilities in order to facilitate the handling of small volumes and use as an electrochemical solvent media without the need of supporting electrolyte, which simplifies the experimental arrangements.

4. Conclusions

In this contribution, the I-V characteristics of two pNIPAAM based IOs and the corresponding pure ILs were investigated employing interdigitated electrodes made of gold. After applying a voltage, an induced current rectification was observed due to the adsorption of the ions onto Au surfaces that generate an accumulation zone. The current rectification behaviour was observed in both IOs and corresponding pure ILs, but the highest rectification ratio was observed for IL-1 (102.47 from $I_{+1\ V}/I_{-1\ V}$). The lower values observed for both IOs in comparison of that obtained for neat ILs were ascribed to the polymeric matrix that probably mitigates ion adsorption.

The stability against oxidation and reduction processes was analyzed by cyclic voltammetry. Due to the hydrophilic character of IL-1, peaks related to water absorption from the atmosphere were found when the samples were left at ambient conditions. This effect narrows the electrochemical window of the IO-1 in comparison to IO-2. IL-2 and IO-2 present wide electrochemical windows, 5.12 V and 3.88 V respectively. These potential windows exceed by far those observed in aqueous electrolytes and are equal or slightly wider than those obtained with organic electrolytes. Moreover, IO-1 presents a suitable matrix for the study of electroactive redox molecules without the need of attaching the ferrocene to the imidazolium center or as a counter ion.

Acknowledgements

This work was supported by the Basque Government under the Elkartek Program (MICRO4FAB, Grant No. KK-2016/00030). N.G.-G. was supported by a PhD fellowship from the University of Navarra. F.B.-L. acknowledges funding support from Gobierno de España, Ministerio de Economia y Competitividad, with Grant No. BIO2016-80417-P and Gobierno Vasco Dpto. Educación for the consolidation of research groups (IT1271-19).

5. References

[1] S. Thiemann, S.J. Sachnov, M. Gruber, F. Gannott, S. Spallek, M. Schweiger, J. Krückel, J. Kaschta, E. Spiecker, P. Wasserscheid, J. Zaumseil, Spray-coatable ionogels based on silane-ionic liquids for low voltage, flexible, electrolyte-gated organic transistors, J. Mater. Chem. C. 2 (2014) 2423–2430. https://doi.org/10.1039/C3TC32465F.

[2] V. Chaudoy, F. Tran Van, M. Deschamps, F. Ghamouss, Ionic liquids in a poly ethylene oxide cross-linked gel polymer as an electrolyte for electrical double layer capacitor, J.

Power Sources. 342 (2017) 872–878. https://doi.org/10.1016/j.jpowsour.2016.12.097.

[3] J. Le Bideau, L. Viau, A. Vioux, Ionogels, ionic liquid based hybrid materials, Chem. Soc. Rev. 40 (2011) 907–925. https://doi.org/10.1039/c0cs00059k.

[4] P. Calvert, Hydrogels for soft machines, Adv. Mater. 21 (2009) 743–756. https://doi.org/10.1002/adma.200800534.

[5] K. Ghandi, A Review of Ionic Liquids, Their Limits and Applications, Green Sustain. Chem. 04 (2014) 44–53. https://doi.org/10.4236/gsc.2014.41008.

[6] M. Czugala, C. O'Connell, C. Blin, P. Fischer, K.J. Fraser, F. Benito-Lopez, D. Diamond, Swelling and shrinking behaviour of photoresponsive phosphonium-based ionogel microstructures, Sensors Actuators, B Chem. 194 (2014) 105–113. https://doi.org/10.1016/j.snb.2013.12.072.

[7] F. Benito-Lopez, M. Antoñana-Díez, V.F. Curto, D. Diamond, V. Castro-López, Modular microfluidic valve structures based on reversible thermoresponsive ionogel actuators, Lab Chip. 14 (2014) 3530–3538. https://doi.org/10.1039/c4lc00568f.

[8] T. Akyazi, J. Saez, J. Elizalde, F. Benito-Lopez, Fluidic flow delay by ionogel passive pumps in microfluidic paper-based analytical devices, Sensors Actuators, B Chem. 233 (2016) 402–408. https://doi.org/10.1016/j.snb.2016.04.116.

[9] T. Akyazi, N. Gil-González, L. Basabe-Desmonts, E. Castaño, M.C. Morant-Miñana, F. Benito-Lopez, Manipulation of fluid flow direction in microfluidic paper-based analytical devices with an ionogel negative passive pump, Sensors Actuators B Chem. 247 (2017) 114–123. https://doi.org/10.1016/j.snb.2017.02.180.

[10] V.F. Curto, C. Fay, S. Coyle, R. Byrne, C. O'Toole, C. Barry, S. Hughes, N. Moyna, D. Diamond, F. Benito-Lopez, Real-time sweat pH monitoring based on a wearable chemical barcode micro-fluidic platform incorporating ionic liquids, Sensors Actuators, B Chem. 171–172 (2012) 1327–1334. https://doi.org/10.1016/j.snb.2012.06.048.

[11] S. Gallagher, A. Kavanagh, B. Ziołkowski, L. Florea, D.R. Macfarlane, K. Fraser, D. Diamond, Ionic liquid modulation of swelling and LCST behavior of N-isopropylacrylamide polymer gels, Phys. Chem. Chem. Phys. 16 (2014) 3610–3616. https://doi.org/10.1039/c3cp53397b.

[12] N. Gil-González, T. Akyazi, E. Castaño, F. Benito-Lopez, M.C. Morant-Miñana, Elucidating the role of the ionic liquid in the actuation behavior of thermo-responsive ionogels, Sensors Actuators B Chem. 260 (2018) 380–387. https://doi.org/10.1016/j.snb.2017.12.153.

[13] N. Gil-González, C. Chen, T. Akyazi, A. Zuzuarregui, A. Rodriguez, M. Knez, E. Castaño, F. Benito-Lopez, M.C. Morant-Miñana, AZO embedded interdigitated electrodes for monitoring stimuli responsive materials, Adv. Funct. Mater. (2018).

[14] C. Liang, C.-Y. Yuan, R.J. Warmack, C.E. Barnes, S. Dai, Ionic Liquids: A New Class of Sensing Materials for Detection of Organic Vapors Based on the Use of a Quartz Crystal Microbalance, Anal. Chem. 74 (2002) 2172–2176. https://doi.org/10.1021/ac011007h.

[15] X. Zhu, H. Zhang, J. Wu, Chemiresistive ionogel sensor array for the detection and discrimination of volatile organic vapor, Sensors Actuators B Chem. 202 (2014) 105–113. https://doi.org/10.1016/j.snb.2014.05.075.

[16] H.M. Upadhyaya, S. Senthilarasu, M.-H. Hsu, D.K. Kumar, Recent progress and the status of dye-sensitised solar cell (DSSC) technology with state-of-the-art conversion efficiencies, Sol. Energy Mater. Sol. Cells. 119 (2013) 291–295. https://doi.org/10.1016/j.solmat.2013.08.031.

[17] M. Salasamendi, L. Rubatat, D. Mecerreyes, Polymeric Ion Gels: Preparation Methods, characterization, and Applications, in: A.A.J. Torriero (Ed.), Electrochem. Ion. Liq. Appl., Burwood, VIC, Australia, 2015: pp. 283–316. https://doi.org/10.1007/978-3-319-15132-8.

[18] I. Osada, H. De Vries, B. Scrosati, S. Passerini, Ionic-Liquid-Based Polymer Electrolytes

for Battery Applications, Angew. Chemie - Int. Ed. 55 (2016) 500–513. https://doi.org/10.1002/anie.201504971.

[19] O.J. Cayre, T.C. Suk, O.D. Velev, Polyelectrolyte diode: Nonlinear current response of a junction between aqueous ionic gels, J. Am. Chem. Soc. 129 (2007) 10801–10806. https://doi.org/10.1021/ja072449z.

[20] E. Alveroglu, Y. Yilmaz, Synthesis of p-and n-type gels doped with ionic charge carriers, Nanoscale Res. Lett. 5 (2010) 559–565. https://doi.org/10.1007/s11671-010-9550-0.

[21] J. Nayak, S.K. Mahadeva, Y. Chen, K.S. Kang, J. Kim, Effect of ionic liquid dispersion on performance of a conducting polymer based Schottky diode, Thin Solid Films. 518 (2010) 5626–5628. https://doi.org/10.1016/j.tsf.2010.05.049.

[22] L. Rojo, I. Castro-Hurtado, M.C. Morant-Miñana, G.G. Mandayo, E. Castaño, Li2CO3 thin films fabricated by sputtering techniques: the role of temperature on their properties, CrystEngComm. 16 (2014) 6033–6038. https://doi.org/10.1039/b000000x.

[23] L. Rojo, I. Castro-Hurtado, M.C. Morant-Miñana, G.G. Mandayo, E. Castaño, Enhanced features of Li2CO3 sputtered thin films induced by thickness and annealing time, CrystEngComm. 17 (2015) 1597–1602.

[24] V.F. Lvovich, C.C. Liu, M.F. Smiechowski, Optimization and fabrication of planar interdigitated impedance sensors for highly resistive non-aqueous industrial fluids, Sensors Actuators, B Chem. 119 (2006) 490–496. https://doi.org/10.1016/j.snb.2006.01.003.

[25] H. Weingärtner, Understanding ionic liquids at the molecular level: Facts, problems, and controversies, Angew. Chemie - Int. Ed. 47 (2008) 654–670. https://doi.org/10.1002/anie.200604951.

[26] A. Arce, E. Rodil, A. Soto, Volumetric and viscosity study for the mixtures of 2-ethoxy-2- methylpropane, ethanol, and 1-ethyl-3-methylimidazolium ethyl sulfate ionic liquid, J.

Chem. Eng. Data. 51 (2006) 1453–1457. https://doi.org/10.1021/je060126x.

[27] K. Shimizu, J.N. Canongia Lopes, A.M.P.S. Gonçalves Da Silva, Ionic Liquid Films at the Water-Air Interface: Langmuir Isotherms of Tetra-alkylphosphonium-Based Ionic Liquids, Langmuir. 31 (2015) 8371–8378. https://doi.org/10.1021/acs.langmuir.5b01977.

[28] M.S. Calado, A.S.H. Branco, J.C.F. Diogo, J.M.N.A. Fareleira, Z.P. Visak, Solubility, volumetric properties and viscosity of the sustainable systems of liquid poly(ethylene glycol) 200 with imidazolium- and phosphonium-based ionic liquids: Cation and anion effects, J. Chem. Thermodyn. 80 (2015) 79–91. https://doi.org/10.1016/j.jct.2014.08.018.

[29] Y.-Z. Su, J.-W. Yan, M.-G. Li, Z.-X. Xie, B.-W. Mao, Z.-Q. Tian, Adsorption of solvent cations on Au(111) and in alkylimidazolium-based ionic liquids-Worm-like versus Micelle-like structures, Zeitschrift Fur Phys. Chemie. 226 (2012) 979–994. https://doi.org/10.1524/zpch.2012.0255.

[30] M. Gnahm, C. Müller, R. Répánszki, T. Pajkossy, D.M. Kolb, The interface between Au(100) and 1-butyl-3-methyl-imidazolium-hexafluorophosphate, Phys. Chem. Chem. Phys. 13 (2011) 11627–11633. https://doi.org/10.1039/c1cp20562e.

[31] X. Zeng, Z. Wang, A. Rehman, Electrode-Electrolyte Interfacial Processes in Ionic Liquids and Sensor Applications, in: A.A.J. Torriero (Ed.), Electrochem. Ion. Liq., Springer New York, Burwood, VIC, Australia, 2015: pp. 7–74. https://doi.org/10.1007/978-3-319-13485-7.

[32] V. V. Singh, A.K. Nigam, A. Batra, M. Boopathi, B. Singh, R. Vijayaraghavan, Applications of ionic liquids in electrochemical sensors and biosensors, Int. J. Electrochem. 2012 (2011) 126–135. https://doi.org/10.1155/2012/165683.

[33] R.F. Carvalhal, R.S. Freire, L.T. Kubota, Polycrystalline gold electrodes: A comparative study of pretreatment procedures used for cleaning and thiol self-assembly monolayer formation, Electroanalysis. 17 (2005) 1251–1259. https://doi.org/10.1002/elan.200403224.

[34] L.D. Burke, P.F. Nugent, The Electrochemistry of Gold : I The Redox Behaviour of the Metal in Aqueous Media, Gold Bull. 30 (1997) 43–53. https://doi.org/10.1007/BF03214756.

[35] J. Xie, T.L. Riechel, Electrochemistry of 1-ethyl-3 methylimidazolium chloride in acetonitrile, J. Electrochem. Soc. 145 (1998) 2660–2664. https://doi.org/10.1149/1.1838696.

[36] B. Gorodetsky, T. Ramnial, N.R. Branda, J.A.C. Clyburne, Electrochemical reduction of an imidazolium cation: a convenient preparation of imidazol-2-ylidenes and their observation in an ionic liquid, Chem. Commun. 0 (2004) 1972–1973. https://doi.org/10.1039/B407386J.

[37] K. Tsunashima, Y. Sakai, M. Matsumiya, Physical and Electrochemical Properties of Room-Temperature Ionic Liquids Containing Allyl-Based Phosphonium Cations and Bis(fluorosulfonyl)amide Anion, ECS Trans. 66 (2015) 33–39. https://doi.org/10.1149/06627.0033ecst.

[38] T.-Y. Wu, S.-G. Su, S.-T. Gung, M.-W. Lin, Y.-C. Lin, C.-A. Lai, I.-W. Sun, Ionic liquids containing an alkyl sulfate group as potential electrolytes, Electrochim. Acta. 55 (2010) 4475–4482. https://doi.org/10.1016/j.electacta.2010.02.089.

[39] M. Hayyan, F.S. Mjalli, M.A. Hashim, I.M. AlNashef, T.X. Mei, Investigating the electrochemical windows of ionic liquids, J. Ind. Eng. Chem. 19 (2013) 106–112. https://doi.org/10.1016/j.jiec.2012.07.011.

[40] The electrochemical stability window has been provided by the ionic liquid supplier, (n.d.).

[41] U. Schröder, J.D. Wadhawan, R.G. Compton, F. Marken, P.A.Z. Suarez, C.S. Consorti, R.F. de Souza, J. Dupont, Water-induced accelerated ion diffusion: voltammetric studies in 1-methyl-3-[2,6-(S)-dimethylocten-2-yl] imidazolium tetrafluoroborate, 1-butyl-3-methylimidazolium tetrafluoroborate and hexafluorophosphate ionic liquids, New J.

Chem. 24 (2000) 1009–1015. https://doi.org/10.1039/b007172m.

[42] C. Zhao, G. Burrell, A.A.J. Torriero, F. Separovic, N.F. Dunlop, D.R. Macfarlane, A.M. Bond, Electrochemistry of Room Temperature Protic Ionic Liquids, J Phys Chem B. 112 (2008) 6923–6936.

[43] S. Bruckenstein, M. Shay, An in situ weighing study of the mechanism for the formation of the adsorbed oxygen monolayer at a gold electrode, J. Electroanal. Chem. 188 (1985) 131–136. https://doi.org/10.1016/S0022-0728(85)80057-7.

[44] D. Bengio, E. Mendes, S. Pellet-Rostaing, P. Moisy, Electrochemical behavior of platinum and gold electrodes in the aprotic ionic liquid N,N-Trimethylbutylammonium Bis(trifluoromethanesulfonyl)imide, J. Electroanal. Chem. 823 (2018) 445–454. https://doi.org/10.1016/j.jelechem.2018.06.034.

[45] C. Zhao, A.M. Bond, X.Y. Lu, Determination of Water in Room Temperature Ionic Liquids by Cathodic Stripping Voltammetry at a Gold Electrode, Anal. Chem. 84 (2012) 2784–2791. https://doi.org/Doi 10.1021/Ac2031173.

[46] Q.-G. Zhang, N.-N. Wang, Z.-W. Yu, The Hydrogen Bonding Interactions between the Ionic Liquid 1-Ethyl-3-Methylimidazolium Ethyl Sulfate and Water, J. Phys. Chem. B. (2010) 4747–4754. https://doi.org/10.1021/jp1009498.

[47] T. Kanematsu, T. Sato, Y. Imai, K. Ute, T. Kitayama, Mutual- and self-diffusion coefficients of a semiflexible polymer in solution, Polym. J. 37 (2005) 65–73. https://doi.org/10.1295/polymj.37.65.

[48] M. Libansky, J. Zima, J. Barek, A. Reznickova, V. Svorcik, H. Dejmkova, Basic electrochemical properties of sputtered gold film electrodes, Electrochim. Acta. 251 (2017) 452–460. https://doi.org/10.1016/j.electacta.2017.08.048.

[49] L.E. Barrosse-Antle, A.M. Bond, R.G. Compton, A.M. O'Mahony, E.I. Rogers, D.S. Silvester, Voltammetry in room temperature ionic liquids: Comparisons and contrasts

with conventional electrochemical solvents., Chem. - An Asian J. 5 (2010) 202–230. https://doi.org/10.1002/asia.200900191.

[50] M.C. Morant-Miñana, J. Elizalde, Microscale electrodes integrated on COP for real sample Campylobacter spp. detection, Biosens. Bioelectron. 70 (2015) 491–497. https://doi.org/10.1016/j.bios.2015.03.063.

[51] D. Zigah, J. Ghilane, C. Lagrost, P. Hapiot, Variations of diffusion coefficients of redox active molecules in room temperature ionic liquids upon electron transfer, J. Phys. Chem. B. 112 (2008) 14952–14958. https://doi.org/10.1021/jp8055625.

[52] R. Balasubramanian, W. Wang, R.W. Murray, Redox ionic liquid phases: Ferrocenated imidazoliums, J. Am. Chem. Soc. 128 (2006) 9994–9995. https://doi.org/10.1021/ja0625327.